Journal of Applied Polymer Science

Acrylic-based epoxy resin damping systems: Synthesis, characterization, and properties

Yuan Yang,[1] Yun-Feng Zhao,[2] Jian-Yue Wang,[2] Chuan Zhao,[2] Liu Tong,[2] Xiao-Yan Liu,[2] Mao-Sheng Zhan[1]

[1]Key Laboratory of Aerospace Materials and Performance (Ministry of Education), School of Materials Science and Engineering, Beihang University, Beijing, China

[2]Aerospace Research Institute of Materials & Processing Technology, Beijing, 100076, China

Correspondence to: Y. Yang (E-mail: yangyuan3001@163.com)

ABSTRACT: Acrylate-based epoxy resin (AE)/low molecular weight polyamine (LPA) composites were developed. The chemical structure, curing behavior, fracture morphology, damping properties, and mechanical properties were evaluated by Fourier transform infrared (FTIR), ^{1}H-nuclear magnetic resonance (^{1}H-NMR), gel permeation chromatography (GPC), Differential scanning calorimeter (DSC), scanning electron microscope (SEM), Dynamic mechanical thermal analysis (DMTA), and electro mechanical machine. Transmission electron microscope (TEM) and SEM pictures exhibited nanoscale micro-phase separation between epoxy and acrylic segmers. DMTA results indicated that the loss factor of cured AE/LPA system could reach 1.84 and temperature range of tan $\delta > 0.5$ was about 84 °C. Tensile strength and elongation at break of the cured AE samples can reach 6.5 MPa and 185%, respectively. © 2016 Wiley Periodicals, Inc. J. Appl. Polym. Sci. **2016**, *133*, 43654.

KEYWORDS: elastomers; manufacturing; mechanical properties; thermosets; viscosity and viscoelasticity

Received 10 September 2015; accepted 15 March 2016

DOI: 10.1002/app.43654

INTRODUCTION

Damping materials are a sort of viscoelastic materials that can be used to control the unwanted vibration and noise through vibration energy dissipation. Therefore, damping materials can be applied on many fields such as aerospace, marine, automobile, construction, and so on.[1,2] Traditional damping materials include rubbers, polyurethane, etc. Generally, viscoelastic polymers were rarely used as composite matrix for their poor flowability and wetting properties with fibers. While, Epoxy resins, due to their excellent chemical resistance, adhesion, dimensional stability, and mechanical properties, are considered as one of the most important classes of thermosetting polymers and find extensive use in various fields of coating, adhesives, electronic-packaging materials, and composites matrix.[3,4] However, the poor damping properties, caused by its high crosslink density, have greatly limited their applications. Recent years, great efforts have been done to modify the damping properties of epoxy resins.[5–8] As reported in reference, flexible resin matrix and flexible curing agent compounds would prepare better damping systems than usual systems.[9] The most common methods to enhance the damping capacity of epoxy resin was through the additions of reinforcing phases, such as rubber,[5,9–11] thermoplastic polymers,[6,12–14] and inorganic fillers,[7,15–17] which can form a multiphase morphology or semi-interpenetrating polymer network.[8,18–20] In this way, vibration energy can be dissipated through phase separation, plastic deformation, and interface friction between fillers or matrix and fillers, and thus the damping properties of epoxy resins can be improved. Besides what is mentioned above, the modification to resin structure, such as incorporating flexible backbone structure, which may decrease the crosslink density of epoxy resin system, will be an effective way to improve its damping intensity. Grant *et al.*[21] used viscoelastic RF-69 as the chain extension modifier to prepare intrinsic epoxy resin damped composites, and the results showed that the damping intensity of the composite improved significantly. Wang *et al.*[22] used amino-terminated polyether and amino-terminated polyurethane as curing agent to prepare a novel flexible epoxy resin system, which showed pretty damping property and the highest value of loss factor reached 1.57. Acrylate polymers showed excellent damping properties[23–25] for plenty of polar ester groups. Extensive studies have been carried out on acrylate polymers, including copolymers,[23] interpenetrating polymer network (IPN),[24] and blends.[25] However, little research was reported on the application of extended modification of epoxy resins.

In this article, we introduced a series of novel acrylate-based epoxy resins (AEs) damping materials, and prepared through a

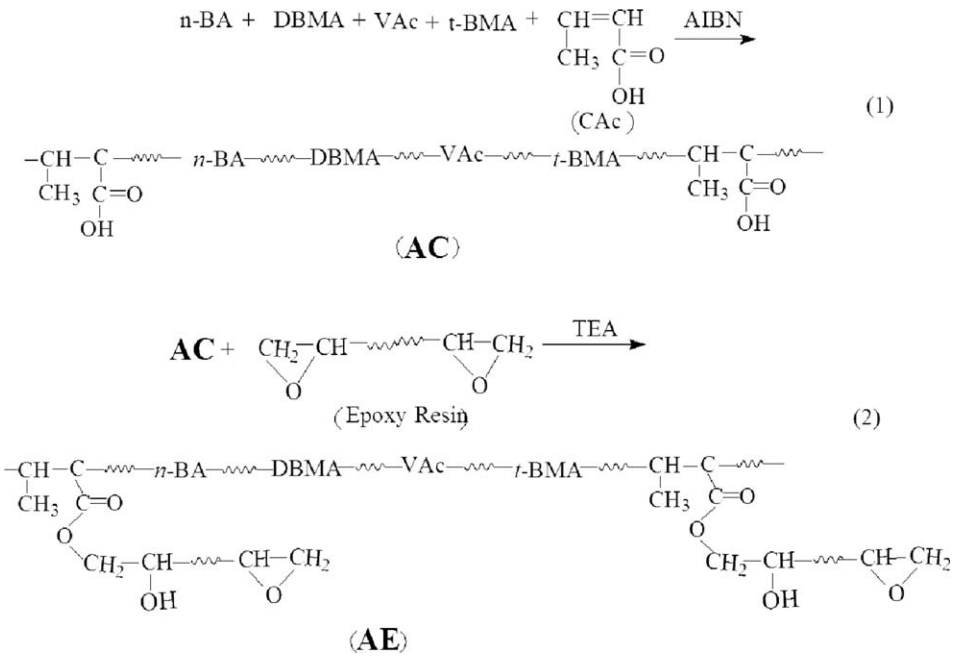

Scheme 1. Reaction scheme of (1) AC and (2) AE.

two-step polymerization method. Then, we prepared a new AEs/ low molecular weight polyamine (LPA) damping materials and the chemical structures, fracture morphology, mechanical, and damping properties were investigated. The damping and mechanical results suggests that AEs is a promising candidate as an epoxy damping matrix.

EXPERIMENTAL

Materials

n-Butyl acrylate (*n*-BA), vinyl acetate (VAc), dibutyl maleate (DBMA), crotonic acid (CAc), and *tert*-butyl methacrylate (*t*-BMA) was supplied by Sinopharm. Azodiisobutyronitrile (AIBN), which was used as initiator, was purchased from Sinopharm (Beijing, China). Triethylamine (TEA), which was used as catalyst for reaction between epoxy groups and carboxyl groups. Low molecular weight polyamide resin (LPA), which supplied by Shanghai Resin Co., Ltd. (China), was used as a curing agent in a weight ratio of 100/50, i.e., 50 phr (parts per hundred epoxy resin). All of the reagents were used as received.

The acrylate based epoxy resin AE was prepared through a two-steps polymerization method, showed in Scheme 1.

Firstly, the ingredients were added into a 500 mL three-neck round-bottom flask equipped with a mechanical stirrer, reflux condenser, and thermometer under nitrogen atmosphere. The mixture was heated to 85 °C, and the reaction was continued for another 1 h to obtain the acrylate prepolymer (AC). The second step was the reaction between epoxy group and carboxyl group. Epoxy resin was added to the above flask and stirred vigorously for 30 min to form a homogeneous liquid blends. Finally, TEA, used as catalytic agent, was added to the flask and the reaction was carried out at 100 °C for 2 h to obtain the acrylate-based epoxy resin (AE).

The acrylate-based epoxy resins with various crotonic acid content were prepared similarly, which were denoted as AE-20, AE-30, and AE-40.

Acrylate-based epoxy resin and curing agent (LPA) in a predetermined weight ratio were charged in a beaker, and stirred for 15 min at room temperature. The epoxy/LPA blends was degassed under reduced pressure for 30 min and then poured into a preheated mold, followed by being cured at 70 °C for 1 h, 100 °C for 1 h, and 130 °C for 2 h, then cooling down to room temperature to obtain the cured samples.

Characterization

Fourier transform infrared (FTIR) spectra of the samples were recorded on a PerkinElmer Spotlight 400 FTIR spectrometer by using the attenuated total reflectance (ATR) method. The spectra were collected from 4000 to 400 cm^{-1}.

^{1}H-nuclear magnetic resonance (^{1}H-NMR) spectra of the samples was recorded on a Bruker V600 spectrometer, and the solvent was $CDCl_3$.

Gel permeation chromatography (GPC, Breeze 2 HPLC system) was used to collect the average molecular weight of AC and AE. A standard sample of polystyrene was used as reference for GPC testing. Tetrahydrofuran (THF) solution of AC and AE was prepared 4 h to make the dissolution completed. Then, the solution (50 mL) was injected into the testing system with a THF elution rate of 1 mL/min at 25 °C. From GPC testing, weight-average molecular weight (*Mw*), Z-average molecular weight (*Mz*), and weight distribution index (defined as *Mz*/*Mw*) can be obtained.

Epoxide values of various AE were characterized through hydrochloric acid–acetone and the testing was taken placed according to GB/T 1677-2008. Hydrochloric acid–acetone solution of AE was prepared 2 h to make the dissolution complete. Then, the

Table I. Recipes for Epoxy-Acrylate Copolymers

	n-BA (g)	DBMA (g)	VAc (g)	CAc (g)	AIBN (g)	EP (g)	TEA (g)
AE-20	45	15	40	20	0.1	91.4	0.4
AE-30	45	15	40	30	0.1	141.3	0.6
AE-40	45	15	40	40	0.1	191.2	0.8

solution was titrated by standard NaOH solution (0.1 mol/L) and epoxide values can be achieved.

A differential scanning calorimeter (DSC, Metteler Toledo DSC 1 Star System) was used for dynamic DSC measurements under N_2 atmosphere. Dynamic DSC measurements were carried out at 5, 10, 15, and 20 °C/min for the uncured AE-20, AE-30, and AE-40/LPA systems.

Morphology of AE samples was performed on a scanning electron microscope (SEM) with an acceleration voltage of 20 kV. The samples were fractured in liquid nitrogen. Before examination, all the fracture surfaces were sputtered coated with gold.

Aggregation structures of AE samples were characterized on a transmission electron microscope (TEM) with an acceleration voltage of 100 kV. The samples were cut into slices by ultra microtome. Before examination, all samples should be dyed by tungstophosphoric acid and the acrylic segmers would be dyed to dead color.

Dynamic mechanical thermal analysis (DMTA) was carried out using a DMTA VA4000 (Metravib R.D.S.) by using a tensile clamp and the testing method of temperature step-frequency sweep with a temperature step of 2 °C and a frequency range between 10 Hz and 100 Hz. The sample dimensions were 20 mm long, 6 mm wide, and 2 mm thick. The storage modulus E', the loss modulus E'', and the loss factor (tan δ) could be obtained from the testing, and the peak temperature of tan δ is taken as the glass transition temperature.

The tensile tests were carried out on an electro-mechanical machine (Sintech65/G, MTS), using dumb-bell shaped type sample. Five samples were tested per material. The hardness was performed on a Shore A durometer. All samples were evaluated without any condition.

RESULTS AND DISCUSSION

Synthesis of Acrylate-Based Epoxy Resin

The two-step synthetic route of acrylate-based epoxy resin was shown in Scheme 1. In the first step, acrylate monomers and AIBN in a predetermined weight ratio, as shown in Table I, were used. The radical polymerization was taken place under the catalysis of AIBN at 90–100 °C for another 1 h when the exothermic was finished and the product was ready for the following reaction. The second step was the esterification reaction between carboxyl groups in acrylate prepolymer and the epoxy groups with a molar ratio of 1:2 at 100 °C for 2 h, which was carried out under the catalysis of TEA to prepare acrylate-based epoxy resin. Part of the epoxy groups participated in the esterification reaction as shown in Scheme 1(2), while the excess epoxy groups could participate in the curing process of the acrylate based epoxy resin.

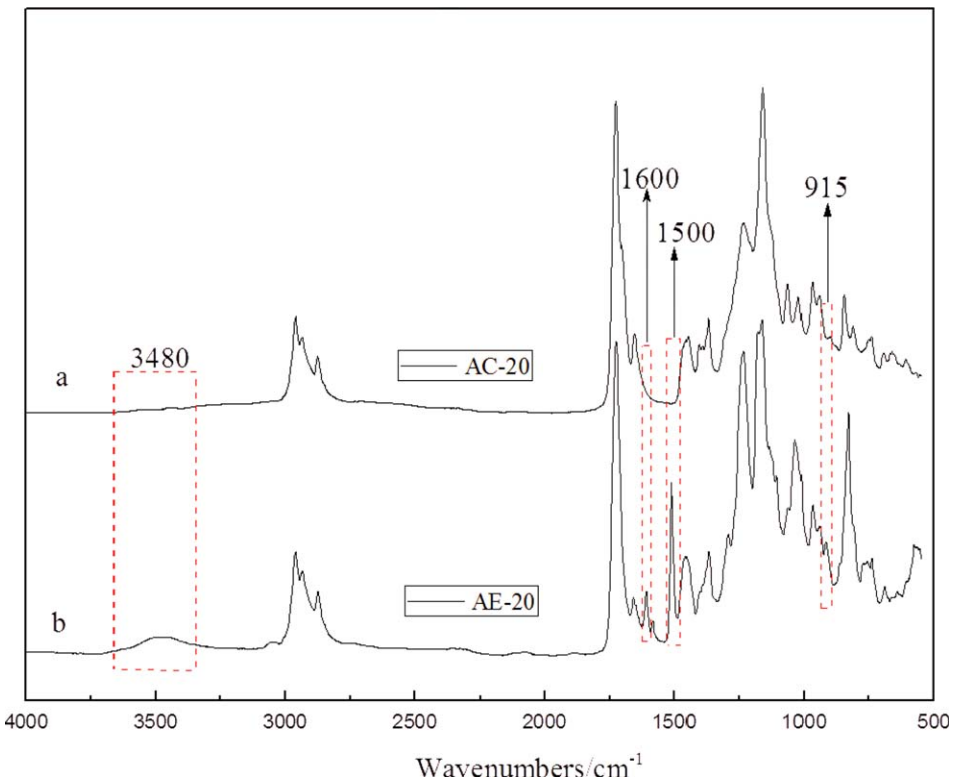

Figure 1. FTIR spectra of reaction product (a) AC; (b) AE. [Color figure can be viewed in the online issue, which is available at wileyonlinelibrary.com.]

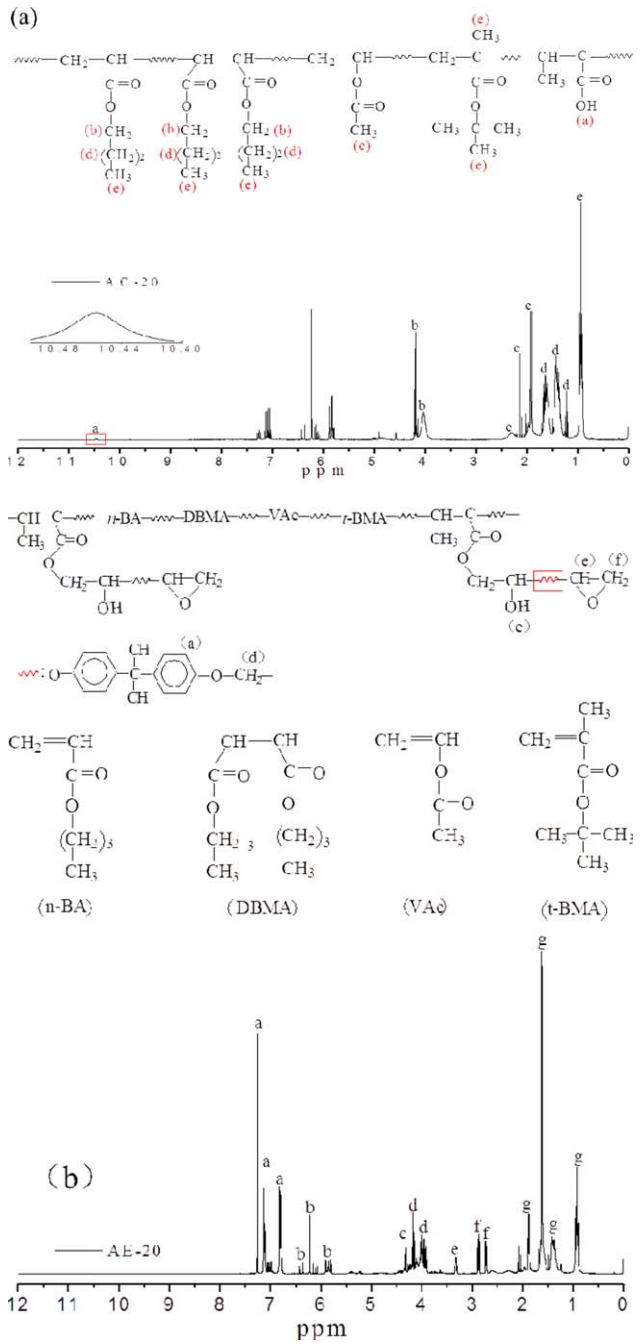

Figure 2. ^{1}H-NMR spectrum of AE. [Color figure can be viewed in the online issue, which is available at wileyonlinelibrary.com.]

FTIR Analysis

FTIR was employed to investigate the chemical structure of epoxy acrylate copolymers. Figure 1 showed the spectrums of the AC and the AE. As shown in Figure 1(a), the bands at 2960–2870 cm^{-1} and 1728 cm^{-1} were assigned to aliphatic –C–H stretching and C = O stretching. Figure 1(b) exhibited the spectra of epoxy acrylate copolymer. The newly emerged bands at 3480 cm^{-1}, 915 cm^{-1}, 1500 cm^{-1}, and 1600 cm^{-1} were corresponding to –O–H stretching, epoxy group, and C = C groups in the aromatic rings of epoxy resin, respectively. The results implied that the epoxy resin was introduced into the copolymer structure.

Table II. Molecular Weight of Various AC and AE

Code	Mw	Mz	Mz/Mw
AC-20	73513	154465	2.101
AC-30	57239	129648	2.265
AC-40	45578	103178	2.263
AE-20	80549	168063	2.086
AE-30	73331	140576	1.917
AE-40	73429	152119	2.071

^{1}H-NMR

The ^{1}H-NMR spectra of the acrylate prepolymer and epoxy acrylate copolymer were shown in Figure 2. As shown in Figure 2(a), the chemical shift at 10.5 ppm is due to the proton on the carboxyl groups. As shown in Figure 2(b), the chemical shift at 4.3 ppm is ascribed to the proton on the hydroxy group, the signals at 4.2 and 3.8 ppm are corresponding to the protons on the methylene (–CH_2–O–Ar); the peak at 3.3 ppm is assigned to CH on the epoxy group; the signals at 2.8 and 2.7 ppm are assigned to CH_2 on the epoxy group; corresponding to Figure 2(a), the chemical shift at 10.5 ppm is disappeared, which means that the esterification between the carboxyl group and epoxide group. The ^{1}H-NMR results further demonstrated that the epoxy resin was introduced into the copolymer structure.

GPC Analysis

Average molecular weight of various AC and AE was characterized through GPC, and the corresponding results were collected in Table II. It was known that both *Mw* and *Mz* for AC decreased gradually with increasing crotonic acid content, which meant a shrinking polymer chain length. For this phenomenon, it can be attributed to the relatively low reactivity of crotonic acid, which was decided by its molecular structure. Comparing to AC prepolymers, the corresponding molecular weight of AE increased significantly. This phenomenon confirmed the reaction between epoxy groups and carboxyl groups, which coincided with FTIR and ^{1}H-NMR results. For all the GPC results, molecular weight distribution index value was around 2, which inferred a relative uniformity for molecular weight distribution.

Epoxide Value Analysis

Epoxide value of AE was characterized through hydrochloric acid–acetone and the corresponding data was collected in Table III. As it can be seen from Table III, the testing epoxide values for various AE were closed to the corresponding theoretical ones. These results also illustrated the reaction between epoxy

Table III. Epoxide Value of Various AE

Code	Theoretical value	Test value
AE-20	0.110	0.12
AE-30	0.127	0.15
AE-40	0.144	0.16

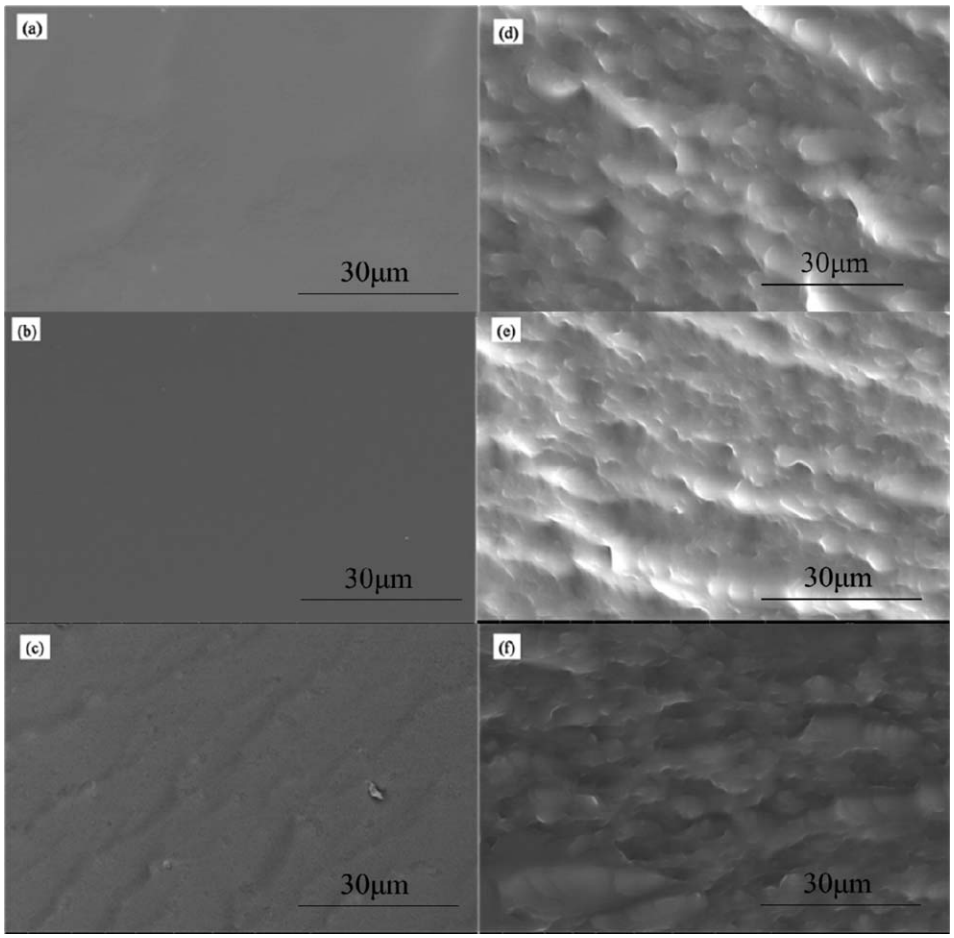

Figure 3. Morphology of AE/LPA systems. (a–c) Surface of frozen break sample for AE-20, AE-30, and AE-40. (d–f) Surface of room temperature break sample for AE-20, AE-30, and AE-40.

groups and carboxyl groups. These results coincided with the FTIR and ^{1}H-NMR spectra.

Curing Behavior

The curing behavior of AE/PLA blends was conducted using a Metteler Toledo DSC 1 Star System instrument. The non-isothermal DSC tests were performed at various heating rate of 5, 10, 15, and 20 °C/min. The dynamic DSC curves of uncured AE/PLA systems were shown in Figure 3. It was observed that there were two exothermic peaks emerged in DSC curves with increasing temperature. It is well known that, exothermic peaks area is associated with the enthalpy of reaction between epoxy groups and curing agent. In Figure 3(a), with the increasing epoxy polymer (EP) content, the height of exothermal peak enhanced, while position of the peaks shifted to lower temperature. For this phenomenon, it might be attributed to the micro-phase separation between EP and acrylate chain. During curing process, the epoxy groups might be trapped in the acrylate phase, which would lead to the decreasing in curing reaction and delayed the exothermal peak position. Increasing epoxide value will improve the content of epoxy group. This meant higher content of epoxy group participated in the curing reaction, which may lead to improvement in the height of exothermal peak and crosslink density.[26–28] In Figure 3(b), position of exothermal peak shifted to higher temperature at higher heating rate. For this phenomenon, it could be attributed to the low thermal conductance and delay in thermal balance of AE polymer, which might lead to the lag of exothermal peak.

Morphology Analysis

The fracture surface micrographs of AE samples were shown in Figure 4. The low temperature fracture micrographs were shown

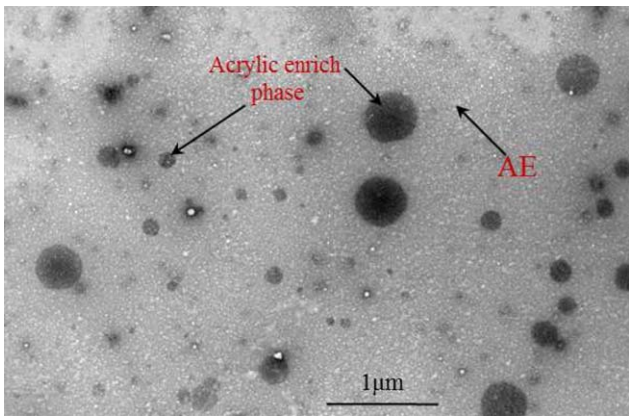

Figure 4. Aggregation structures of AE-40/LPA system. [Color figure can be viewed in the online issue, which is available at www.wileyonlinelibrary.com.]

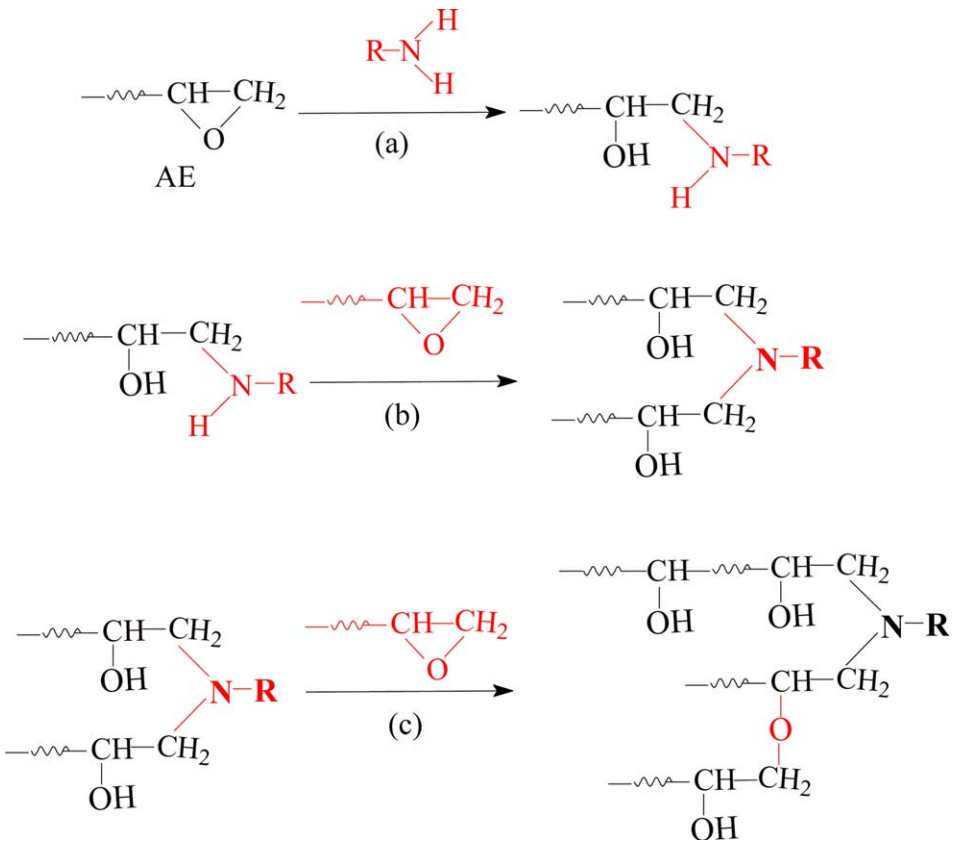

Scheme 2. Curing mechanism of AE/LPA systems. [Color figure can be viewed in the online issue, which is available at wileyonlinelibrary.com.]

in Figure 4(a–c), and the room temperature fracture surface micrographs shown in Figure 4(d–f). It can be seen from Figure 4(a–c), there was no significant plastic deformation and phase separation, which showed a clear fragile morphology. This phenomenon indicated that the AE systems at different content of EP exhibited a homogeneous phase. On the contrary, from Figure 4(d–f), cellular phase structures were observed for all room temperature fracture surface, which was composed by significant shear yielding and corresponding holes. These results might be attributed to the quasi co-continuous phase structure comprised of soft segments (acrylate chain) and hard segments (EP component). Just as shown in Scheme 2, the AE/LPA systems formed crosslink network based on the acrylate chain and epoxy resin component. The incompatibility might lead to slight phase separation between EP and acrylate polymers during curing process, which can be confirmed by the TEM and SEM pictures. While the molecular structure of AE (Scheme 1) restricted the evolution of the phase separation size, which led to the homogeneous structure at macroscopic scale.[29,30]

Aggregation structures of AE samples were characterized on a TEM and the corresponding picture was illustrated in Figure 5. It can be seen from Figure 5, tint area was attributed to AE matrix, on the contrary, dead color area was corresponding to acrylic sigmers enrich phase. Acrylic segmers enrich phase will

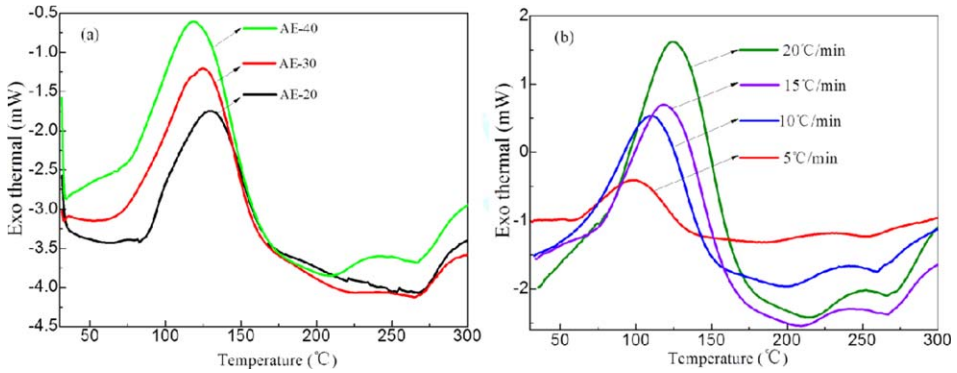

Figure 5. DSC curves of (a) various AEs with a heating rate of 5 °C/min; (b) AE-40/LPA at various heating rate. [Color figure can be viewed in the online issue, which is available at wileyonlinelibrary.com.]

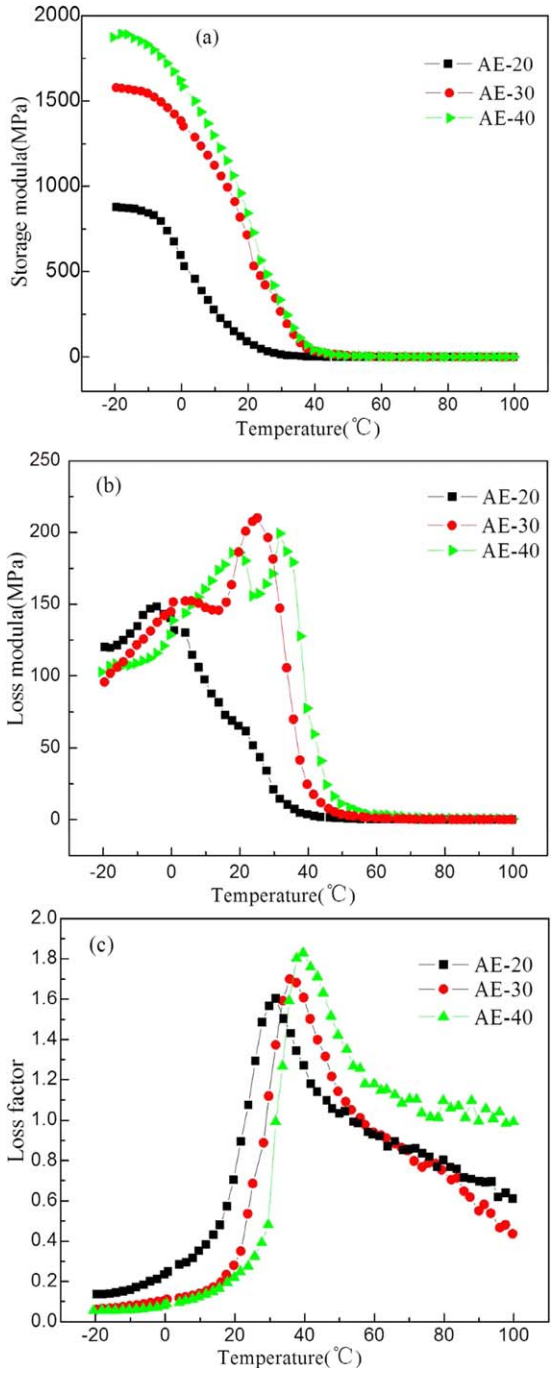

Figure 6. DMTA plots of AE/LPA system. [Color figure can be viewed in the online issue, which is available at wileyonlinelibrary.com.]

form plenty of spherical area with diameter of nanoscale. This result confirmed the micro phase separation between epoxy segmers and acrylic segmers during curing process, whose size might be restricted by the molecular structure of AE (shown in Scheme 1). This result of TEM coincides with the SEM results.

Dynamic Mechanical Thermal Properties

The dynamic mechanical property of AE systems was determined by DMTA. E', E'', and tan δ of AE samples as a function of temperature were listed in Figure 6. As shown in Figure 6(a), the E' enhanced significantly with increasing EP content. The plots for E'' dependent on temperature were illustrated in Figure 6(b). From Figure 6(b), it was clear that there were two peaks in the E'' curves. The peaks at lower temperature corresponded to the acrylate component, while the higher one corresponding to the EP component. Figure 6(c) showed the temperature dependence of tan δ for AE with various EP content. From Figure 6(c), it was clear that there was only one loss factor peak in tan δ curves, indicating a homogeneous phase in macroscopic scale. It can be known that E'' curves showed a phase separation, while the loss factor curves showed a homogeneous phase structure. This phenomenon could be explained by the nanoscale micro phase separation between epoxy segmers and acrylic segmers, which led to the homogeneous structures at macro scale, while phase separation at micro scale. These results could be confirmed by the SEM (Figure 4) and TEM pictures (Figure 5). With the increasing EP content, the glass transition temperature (T_g) around the loss factor peak shifted to higher temperature, and the height of loss factor peaks increased from 1.62 to 1.85, gradually. At the same time, the temperature range (tan $\delta > 0.5$) for AE-20, AE-30, and AE-40 maintained at 70–84 °C. This phenomenon can be attributed to the following aspects. Firstly, the plenty of polar ester groups in acrylate frameworks played an important role in improving the damping performance according to group contribution theory.[31,32] Secondly, as shown in GPC and epoxy value results, the increasing crotonic acid content resulted in the shrinkage of acrylic polymer chain length and improvement on epoxy value. Both of the results will increase the crosslink density of AE/LPA systems. This will constrain movements in chain segments and cause the T_g shifted to higher temperature and decreased $\triangle T$.

Figure 7 showed the temperature dependence of tan δ for AE-40/LPA systems at various frequencies. From Figure 7(a), there was no obviously difference in E'' at various testing frequencies. As shown in Figure 7(c), it was clear that a single tan δ peak was exhibited at about 45 °C, shifted to higher temperature with the increasing testing frequency. This phenomenon can be explained by temperature–frequency superposition (TFS) principle,[33,34] that is to say the effect of increasing temperature on dynamic mechanical properties is equivalent to that of lower test frequency, and vice versa. Similar researches have been reported in reference.[35,36]

Mechanical Properties

The mechanical properties of AE systems was determined by tensile tester and Shore durometer, and tensile strength, elongation at break, and hardness could be obtained. The results were collected in Table IV, and the curves of stress–strain were illustrated in Figure 8. The tensile strength of AE systems increased from 3.0 MPa to 6.5 MPa with the increasing EP content. At the same time, the hardness of the AE systems increased from 46 to 93, while the elongation at break decreased from 290.7% to 185.1% with the increasing EP content. As shown in Figure 8, a linear behavior can be observed for the elastic region, and then followed by an obvious non-linear behavior for plastic region. These results exhibited excellent flexibility. The curves showed a steep increasing behavior during the elastic region. After a yield, the curves showed a gently increase up to a

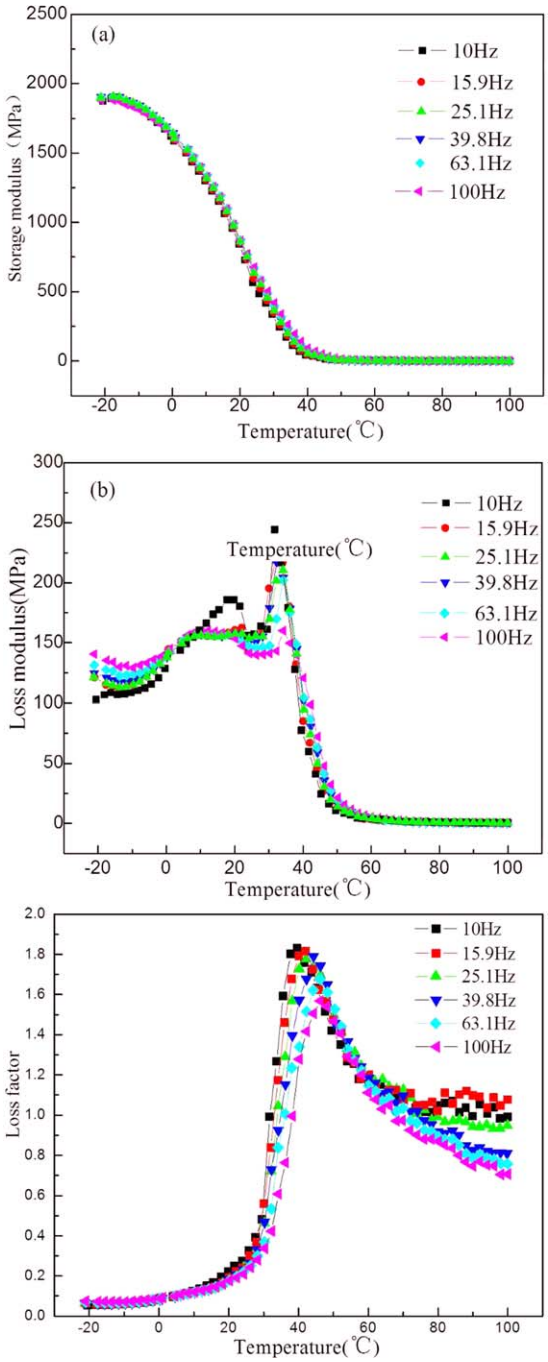

Figure 7. DMTA curves of AE-40/LPA system at various testing frequencies. [Color figure can be viewed in the online issue, which is available at www.wileyonlinelibrary.com.]

sudden failure. With increasing EP content, the yield point increased, while the strain shrunk, gradually. From GPC and epoxy value results, the AEs showed a decrease in the acrylate polymer chain length and improvement on content of epoxy group, which may increase the crosslink density. In addition, the improvement on crosslink density will enhance the mechanical properties including tensile strength and hardness. Moreover, the higher content of epoxy group led to efficient enhancement on the tensile strength and hardness. On the contrary, the higher crosslink density might constrain the motion ability of molecular chain, which led to the decrease of elongation at break.

Table IV. Mechanical Properties Cured AE Systems

Samples	Tensile strength (MPa)	Elongation at break (%)	Hardness
AE-20	3.0	290.7	46
AE-30	5.4	243.4	88
AE-40	6.5	185.1	93

CONCLUSIONS

In this article, the acrylate-based epoxy resins have been successfully prepared through a simple two-step method. Then we prepared AEs/LPA damping materials. The chemical structure, fracture morphology, curing behavior, damping, and mechanical properties of the AE/LPA systems were investigated. The non-isothermal DSC indicated that the main curing process performed at about 100 °C, while the reaction between epoxy groups and hydroxy groups might take place at elevated temperature. The TEM and SEM results indicated a nanoscale microphase separation between EP and acrylic segmers. DMTA results showed that the AE samples exhibited excellent damping properties, with a highest loss factor value of 1.84, and temperature range (tan $\delta > 0.5$) was about 84 °C. At the same time, the tensile strength of the samples ranged from 3.0 to 6.5 MPa, while the elongation at break of all the samples was more than 185%. Though with excellent damping and mechanical properties, T_g of the AE systems is above room temperature, at which the damping management is needed. This may limited its application and further researches should be carried out to resolve above problems. In a word, the acrylate-based epoxy resin, with excellent damping property and high flexibility, shows significant potential as novel and effective damping materials.

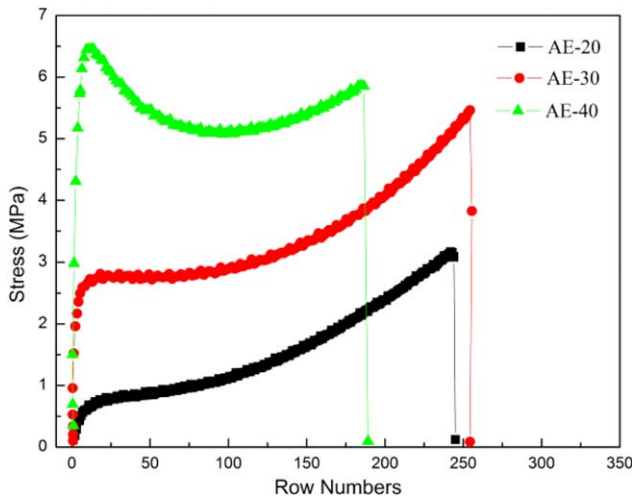

Figure 8. Stress–strain curves of AE/LPA systems. [Color figure can be viewed in the online issue, which is available at wileyonlinelibrary.com.]

ACKNOWLEDGMENTS

Authors would like to gratefully acknowledge supports of careful revision of English from Lifang Zhang, measurements of DMTA from Zhiying Zhang, and the SEM and TEM characterization from Dr. Zhou Peng.

REFERENCES

1. Nikhil, K.; Bingqing, W.; Ajayan, P. M. *Adv. Mater.* **2002**, *14*, 13.
2. Wang, Y.; Zhan, M.; Li, Y.; Shi, M.; Huang, Z. *Polym. Plast. Tech. Eng.* **2012**, *51*, 840.
3. Haris, A. *J. Mater. Sci.* **2008**, *43*, 3289.
4. Wang, G.; Jiang, G.; Zhang, J. *Thermochim. Acta* **2014**, *589*, 197.
5. Tripathi, G.; Srivastava, D. *Mater. Sci. Eng. A* **2007**, *443*, 262.
6. Ji-Fang, F.; Li-Yi, S.; Shuai, Y.; Qing-Dong, Z.; Deng-Song, Z.; Yi, C.; Jun, W. *Polym. Adv. Technol.* **2008**, *19*, 1597.,
7. Gu, J.; Wu, G.; Zhang, Q. *Mater. Sci. Eng. A* **2007**, *452–453*, 614.
8. Tingmei, W.; Shoubing, C.; Qihua, W.; Xianqiang, P. *Mater. Des.* **2010**, *31*, 3810.
9. Hengshi, Z.; Xiaoxue, S.; Xu, S. *J. Appl. Polym. Sci.* **2014**, *131*, 547.
10. Poornima, V. P.; Puglia, D.; Maria, H. J.; Kenny, J. M.; Thomas, S. *RSC Adv.* **2013**, *3*, 24634.
11. Timothy, W. S.; Ketan, S. K.; Mir, K.; Joseph, L. L.; Jan, W. A.; Gregory, B. M.; Rajesh, K. *Soft Matter* **2013**, *9*, 3589.
12. Tang, B.; Liu, X.; Zhao, X.; Zhang, J. *J. Appl. Polym. Sci.* **2014**, DOI: 10.1002/app.40614.
13. Jia-Bin, D.; Hsu-Chiang, K.; Xu-Shen, D. *Polym. Int.* **2009**, *58*, 838.
14. Chen, S.-b.; Wang, Q.-h.; Wang, T.-m. *Polym. Test.* **2011**, *30*, 726.
15. Lu, S.; Li, S.; Yu, J.; Yuan, Z.; Qi, B. *RSC Adv.* **2013**, *3*, 8915.
16. Yang, C.; Dingyang, Y.; Huawei, Z.; Mei, L. *RSC Adv.* **2014**, *4*, 44750.
17. Alnefaie, K. A.; Aldousari, S. M.; Khashaba, U. A. *Compos. Part A* **2013**, *52*, 1.
18. Chern, Y. C.; Tseng, S. M.; Hsieh, K. H. *J. Appl. Polym. Sci.* **1999**, *74*, 328.
19. Shoubing, C.; Qihua, W.; Tingmei, W.; Xianqiang, P. *Mater. Des.* **2011**, *32*, 803.
20. Wenwen, Y.; Dezhi, Z.; Miao, D. *Eur. Polym. J.* **2013**, *49*, 1731.
21. Grant, I. D.; Lowe, A. T.; Thomas, S. *Compos. Struct.* **1997**, *38*, 581.
22. Wang, X.; Liu, H.; Yang, S. *J. Wuhan Univ. Technol. Mater. Sci. Ed.* **2008**, *23*(3): 411.
23. Minri, L.; Zhen, Z.; Liu, S.; Wei, W.; Xiuling, W. *J. Appl. Polym. Sci.* **2010**, *118*, 3203.
24. Su, C.; Zong, D.; Xu, L.; Zhang, C. *J. Appl. Polym. Sci.* **2014**, *131*, 742.
25. Borah, J. S.; Chaki, T. K. *J. Polym. Res.* **2011**, *18*, 569.
26. Francis, B.; Lakshmana Rao, V.; Vanden Poel, G. *Polymers* **2006**, *47*, 5411.
27. Omrani, A.; Simon, L. C.; Rostami, A. A. *Euro. Polym. J.* **2008**, *44*, 769.
28. Nakka, J. S.; Jansen, K. M. B.; Ernst, L. J. *J. Appl. Polym. Sci.* **2013**, 3794.
29. Lipatov, Y. S.; Alekseeva, T. T. *Adv. Polym. Sci.* **2007**, *208*, 1.
30. Xiao-xue, S.; Wen-jia, S.; Ji-chun, Y.; Li-ping, Z.; Xiao-jun, C.; Wen-yong, D.; Yong-jin, L. *Acta Polym. Sin.* **2012**, *11*, 1234.
31. Chang, M. C. O.; Thomas, D. A.; Sperling, L. H. *J. Polym. Sci. B: Polym. Phys.* **1988**, *26*, 1627.
32. Thomas, D. A.; Sperling, L. H. *J. Appl. Polym. Sci.* **1987**, *34*, 409.
33. Xiaojun, H.; Jinrong, W.; Guangsu, H.; Xiaoan, W. *J. Macro. Sci. B: Phys.* **2011**, *50*, 188.
34. Zhang, R.; He, X.; Huang, G. *J. Polym. Res.* **2014**, *21*, 388.
35. Çakır Çanaka, T.; Kayab, K.; Serhatlı, I. E. *Progr. Org. Coat.* **2014**, *77*, 1911.
36. Shi, X.; Li, Q.; Zheng, A. *Polym. Test.* **2014**, *35*, 87.